

# Accuracy of the discrete dipole approximation for simulation of optical properties of gold nanoparticles

Maxim A. Yurkin,<sup>a,b</sup> David de Kanter,<sup>c</sup> and Alfons G. Hoekstra<sup>c</sup>

<sup>a</sup> Institute of Chemical Kinetics and Combustion SB RAS, Institutskaya 3, 630090, Novosibirsk, Russia

<sup>b</sup> Novosibirsk State University, Pirogova 2, 630090, Novosibirsk, Russia

<sup>c</sup> University of Amsterdam, Faculty of Science, Computational Science Research Group, Science Park 107, 1098 XG, Amsterdam, The Netherlands  
A.G.Hoekstra@uva.nl

**Abstract.** We studied the accuracy of the discrete dipole approximation (DDA) for simulations of absorption and scattering spectra by gold nanoparticles (spheres, cubes, and rods ranging in size from 10 to 100 nm). We varied the dipole resolution and applied two DDA formulations, employing the standard lattice dispersion relation (LDR) and the relatively new filtered coupled dipoles (FCD) approach. The DDA with moderate dipole resolutions is sufficiently accurate for scattering efficiencies or positions of spectral peaks, but very inaccurate for e.g. values of absorption efficiencies in the near-IR. To keep relative errors of the latter within 10% about  $10^7$  dipoles per sphere are required. Surprisingly, errors for cubes are about 10 times smaller than that for spheres or rods, which we explain in terms of shape errors. The FCD is generally more accurate and leads to up to 2 times faster computations than the LDR. Therefore, we recommend FCD as the DDA formulation of choice for gold and other metallic nanoparticles.

**Keywords:** discrete dipole approximation, gold nanoparticles, absorption, scattering, simulation, accuracy.

## 1 INTRODUCTION

Plasmon resonance in metal nanoparticles has gained increasing interest in recent years [1-4]. Applications of these nanoparticles are based on their ability to concentrate electromagnetic energy into subwavelength regions and include surface-enhanced Raman scattering [5] and fluorescence [6,7]. In biological applications nanoparticles are conjugated with different molecules, which allow them to be localized in particular biological cells or compartments when introduced into a sample or a tissue [1]. This localization is further used for specific imaging [8] and photodestruction [9], as well as for sensing local chemical environment [10]. Development in this field is pushed by many different methods to produce nanoparticles of different size, shape, and composition, based on chemical synthesis [2,11] or nanolithography [12,13].

Simulation of interaction of light with nanoparticles is an important part of the scientific progress [1,3,14-16]. It is used to both validate existing nanostructures and to aid design of new ones with specific properties. Several methods can be used for particles of arbitrary shapes: the boundary element (surface-integral equation) method [17,18], the null-field method with discrete sources [19,20], the finite difference time domain method [21], and the discrete dipole approximation (DDA) [22-24]. The latter is widely used for simulation of optical properties of gold nanoparticles, due to its versatility and public availability of efficient computer implementations [25,26]. Moreover, the DDA can be used for particles in complex environments, such as particles near a surface [7,27-29] and arrays of nanoparticles [30-32].

Agreement between the DDA simulations and experiments for extinction spectra of gold nanoparticles has never been perfect [22,33,34]. However, the disagreement is attributed mostly to uncertainties in particle shape [33,34] and in the gold refractive index [22]. Moreover, researchers are mainly interested in position of resonance peaks in the spectrum. For instance, "excellent agreement" is stated [35] when peak position is accurately described but extinction values at particular wavelengths disagree by a factor of two.

The accuracy of the DDA itself for scattering of light by gold nanoparticles is usually quoted as "good enough if a large enough number of dipoles is used", i.e. the discussion is qualitative with no error measurements available [36-39]. The fraction of surface dipoles has been discussed as a criterion of DDA accuracy [36,40]. However, this has little predictive power except for general trends that accuracy improves with increasing number of dipoles. In a couple of papers DDA results are plotted together with exact reference results in the same graph for spheres [37] and spheroids [38]. These graphs show that errors of extinction efficiency at particular wavelengths can be as large as 50%. Moreover, a reliable identification of small side peaks in the spectrum is hampered by DDA errors [37]. Similar results have been obtained for silver nanospheres [14].

Although DDA simulations for nanoparticles mostly focus on extinction efficiency, as this is usually measured experimentally, several researchers have studied its constituents – absorption and scattering efficiencies – separately [38,40,41]. This should result in a better understanding of DDA errors, especially their size dependence. Moreover, absorption efficiency is relevant to practical applications involving optical heating of nanoparticles. It is also important to note that all papers mentioned above used the lattice dispersion relation (LDR, [42]) formulation of the DDA or its modification [43]. Other formulations for DDA, e.g. filtered coupled dipoles (FCD, [44]) or integrated Green's tensor [45] may be more suitable for the metallic refractive indices [46]. However, to the best of our knowledge, they have never been tested for such refractive indices, except Ref. 47.

In this manuscript we report on DDA accuracy for simulations of light scattering by gold nanoparticles. We chose three particle shapes (a sphere, a cube, and a rod) and two sizes (10-100 nm) and computed absorption and scattering spectra, using a range of discretizations (number of dipoles) and two DDA formulations (FCD and LDR). We show graphs of relative errors of calculated quantities versus wavelength, as well as errors of position and amplitude of the main spectral peak. The DDA formulations are not only compared in terms of accuracy, but also in terms of computational time.

## 2 METHODS

### 2.1. Model particles

We considered the following gold particles: two spheres (diameters  $D = 10$  and  $100$  nm), two cubes (edge sizes  $D = 10$  and  $100$  nm), and a rod (cylinder with hemispherical caps, diameter  $20$  nm, total length  $90$  nm). The incident light propagates along the  $z$ -axis and is polarized (E-field) along the  $x$ -axis. Cubes are oriented with edges along the coordinate axes, and the rod is oriented with symmetry axis along the  $x$ -axis. While this does not represent the most usual experimental condition (as random orientation), it emphasizes the longitudinal plasmon resonance.

The refractive index of gold nanoparticles is a controversial issue [22]. However, although the specific values of the bulk refractive index (and size corrections to account for surface damping) will have a significant impact on simulation results, they are too small to significantly alter the DDA accuracy (as long as the same refractive index is used for the DDA and the reference method – data not shown). Therefore, we used data for bulk refractive index by Johnson and Christy [48] without size corrections in the wavelength range

[0.398,0.822]  $\mu\text{m}$ . Additionally we interpolated these data near the spectral peaks to improve spectral resolution down to 5 nm.

We consider all our test particles in vacuum. This causes our simulated spectra to look different (in particular, peaks are blue-shifted) from the ones most often found in the literature, when gold particles are suspended in water. Although our choice may lead to certain exaggeration of the problems with DDA accuracy, our results are still general enough and can be applied to particles in water by rescaling wavelength and refractive index. Moreover, some of our results may be interesting *per se* in applications involving nanoparticles deposited on surfaces in air.

## 2.2. Simulation methods

The DDA is a general method to compute scattering and absorption of electromagnetic waves by particles of arbitrary geometry and composition. It solves the Maxwell equations in the frequency domain employing volume discretization. Initially the DDA (sometimes referred to as the "coupled dipole approximation") was proposed by Purcell and Pennypacker (PP) [49], who replaced the scatterer by a set of point dipoles. These dipoles interact with each other and the incident field, giving rise to a system of linear equations, which is solved to obtain dipole polarizations. All the measured scattering quantities can be obtained from these polarizations. This approach was further developed by Draine and coworkers, who popularized the method by developing a publicly available computer code (see e.g. [50]). The DDA can also be derived from the integral equation for the electric field, which is discretized by dividing the scatterer into small cubical subvolumes [51]. However, the final equations, produced by both lines of derivation of the DDA, are essentially the same. An extensive review of DDA, including both theoretical and computational aspects, was recently performed by Yurkin and Hoekstra [46].

As a numerical implementation of the DDA we used ADDA v.0.79 [25], which is capable of running on a cluster of computers parallelizing a single DDA computation [52]. We used two DDA formulations: the LDR [42] and the FCD [44]. A thorough discussion of the FCD and its implementation in ADDA is given in a separate paper [47], while here we only evaluate FCD performance for gold nanoparticles. We used the default iterative solver in ADDA (quasi minimal residual – QMR [53]) and set the stopping criterion to  $10^{-10}$ . This was done to eliminate any possible influence of this value on final results, e.g. when DDA accuracy is very good. Note however that the default value of  $10^{-5}$  is sufficient for most practical applications. Acknowledging the latter fact we use the  $10^{-5}$  threshold when analyzing the required number of iterations for convergence, which is directly connected to computation time (see Fig. 5). We employed volume correction (a default option in ADDA), which ensures that the dipole discretization of the particle has the correct volume. This is not expected to significantly influence results, especially for fine discretizations [52]. All DDA simulations were performed on the Dutch compute cluster LISA [54].

We varied the number of dipoles to discretize the particle shape over a wide range. Common criteria, defined in terms of dipole size parameter or number of dipoles per wavelength, are no longer relevant for DDA simulations of nanoparticles. Instead we use the number of dipoles along the  $x$ -axis ( $n_x$ ) as a measure of discretization.  $n_x$  was varied in the range 16-256, 8-64, and 72-576 for spheres, cubes, and rods respectively. The number of dipoles per rod diameter ( $n_z$ ) was varied from 16 to 128. The largest number of dipoles per particle was  $9 \times 10^6$  requiring 8 GB of RAM.

To obtain reference results for spheres we used the Mie theory. The relative accuracy of the Mie code that we used is at least  $10^{-6}$  [55]. For the rods we employed the T-matrix code by Mishchenko [56,57] modified to calculate extinction and scattering cross sections for particles in a fixed orientation. Elongated gold nanorods are on the edge of the code's applicability (even using extended precision arithmetic), therefore it is hard to put exact

numbers on the T-matrix accuracy. However, based on the convergence behavior of T-matrix results with increasing order of multipoles (data not shown) the relative accuracy is expected to be better than 1%.

To the best of our knowledge no freely available code based on analytical or semi-analytical methods, such as the T-matrix method, exists to accurately simulate light scattering by cubes smaller than wavelength. Therefore, we used an extrapolation technique of the DDA results. In short, several DDA simulations for the same particle are performed, varying only the level of discretization. Then the measured quantity of interest is plotted versus dipole size and is extrapolated to zero dipole size using a second order polynomial. All details together with a theoretical foundation are described elsewhere [58]. This technique provides not only the reference results but also estimates of errors on those results. Extrapolation is based on simulations of light scattering by cubes with  $n_x = 64, 80, 96, 112,$  and  $128$  using the LDR. Convergence of the FCD with refining discretization is less smooth and hence requires further study to be used for extrapolation [47]. Estimates of the extrapolation errors are shown in Fig. 3.

### 3 RESULTS AND DISCUSSION

The reference spectra for all test particles studied in this manuscript are shown in Fig. 1. They were calculated with methods described in Sec. 2.2. Spectral peaks for spheres and cubes are located between 500 and 600 nm, while peaks for a rod are shifted to about 720 nm. One can also see that scattering efficiency ( $Q_{\text{sca}}$ ) is much smaller than absorption efficiency ( $Q_{\text{abs}}$ ) for 10 nm particles and to a lesser extent for a rod, but is comparable to absorption for 100 nm particles. We discuss this further at the end of this section. In the following we analyze relative errors of the DDA for all five test particles and consider separately absorption and scattering efficiencies, because these two scattering quantities show markedly different behavior.

Accuracy results for the spheres are shown in Fig. 2. In the sequel we consider only absolute values of relative errors. Moreover, we show results of several discretizations (characterized by  $n_x$ ) using the FCD and only two discretizations using the LDR. We consider FCD more suitable for simulating light scattering by gold nanoparticles, while two different discretizations are enough to assess the difference between LDR and FCD. We assume that 10% is a typical desired accuracy for absorption and scattering efficiency, although it surely depends on the particular application. The errors are relatively small for wavelengths smaller than about 550 nm, where spectral peaks are located, but quickly increase for larger wavelengths. There is a large difference between accuracy of  $Q_{\text{abs}}$  and  $Q_{\text{sca}}$ .  $n_x = 32$  is generally enough for 10% accuracy of  $Q_{\text{sca}}$  over the whole wavelength range for both FCD and LDR, but even the highest used discretization  $n_x = 256$  (FCD) leads only to 10-20% accuracy of  $Q_{\text{abs}}$  in the near-IR range. The influence of size is moderate: errors for 100 nm are generally 10-30% larger than that for 10 nm. The LDR is less accurate for  $Q_{\text{abs}}$  than the FCD (up to two times), but is slightly more accurate for  $Q_{\text{sca}}$ .

Results for the cubes are shown in Fig. 3, also showing the estimated errors of reference spectra obtained by the extrapolation technique (see Sec. 2.2). The general tendencies of increasing errors with wavelength, a much better accuracy of  $Q_{\text{sca}}$  than that of  $Q_{\text{abs}}$ , and the size influence are the same as for spheres. The behavior of the LDR vs. the FCD is somewhat different. The LDR is comparable to the FCD for  $Q_{\text{abs}}$  (more accurate  $n_x = 16$  but less accurate for  $n_x = 64$ ), but is clearly less accurate for  $Q_{\text{sca}}$ . However, the largest difference between the cubes and the spheres is the remarkably smaller value of the errors. It is smaller by a factor of 10 for the same  $n_x$ . In other words,  $n_x = 32$  (FCD) is enough for 10% accuracy of  $Q_{\text{abs}}$ , and  $n_x$  as small as 8 leads to only several percent error in  $Q_{\text{sca}}$ . This shape effect is further discussed below.

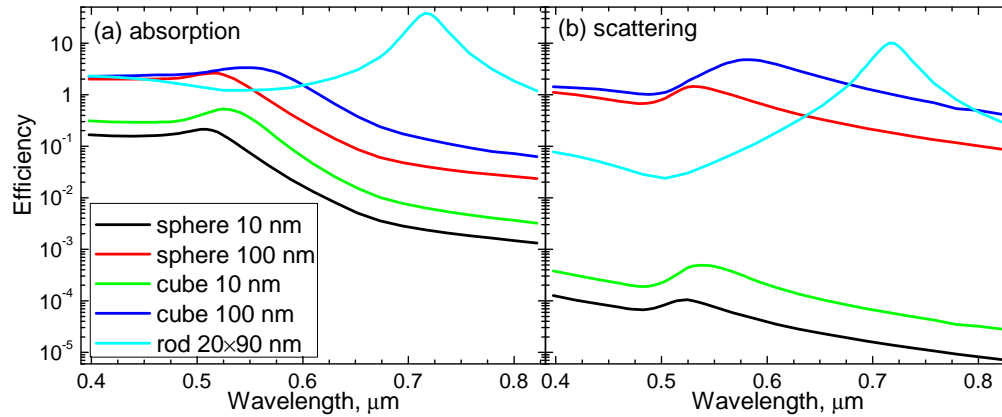


Fig. 1. Reference absorption (a) and scattering (b) spectra in logarithmic scale for all five test particles used in this manuscript (see text).

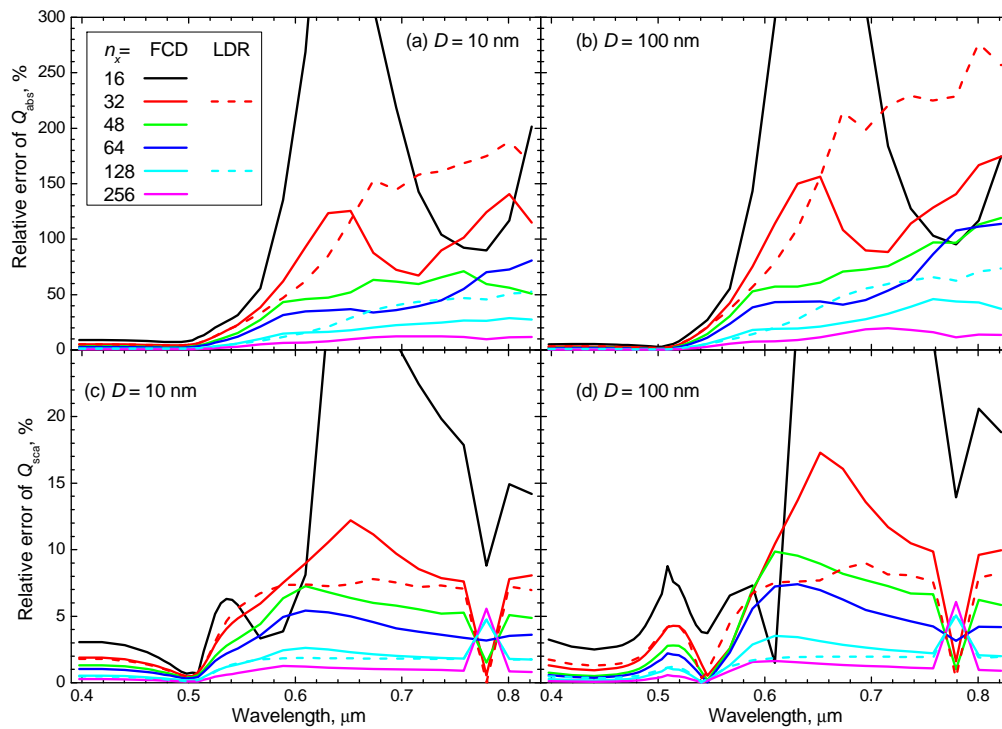


Fig. 2. Relative errors of  $Q_{\text{abs}}$  (a, b) and  $Q_{\text{sca}}$  (c, d) computed using the FCD and LDR formulations of the DDA, varying the number of dipoles, for gold spheres with diameter 10 nm (a, c) and 100 nm (b, d).

Our choice of a rod as the last test particle is based on position of its spectral peaks in the near-IR and its intermediate shape between spheres and cubes. The latter can be explained by considering two factors of the influence of particle shape on the DDA accuracy. The first factor is whether the particle shape can or cannot be precisely described by a set of cubical dipoles. The errors are expected to be generally larger for the latter particles due to the shape errors [58]. The second factor is the notion that "spheres are special" [59], i.e. the results for spheres (both scattering quantities themselves and their errors when simulated with DDA) are markedly different from most other shapes. In the Rayleigh domain, this can be explained by

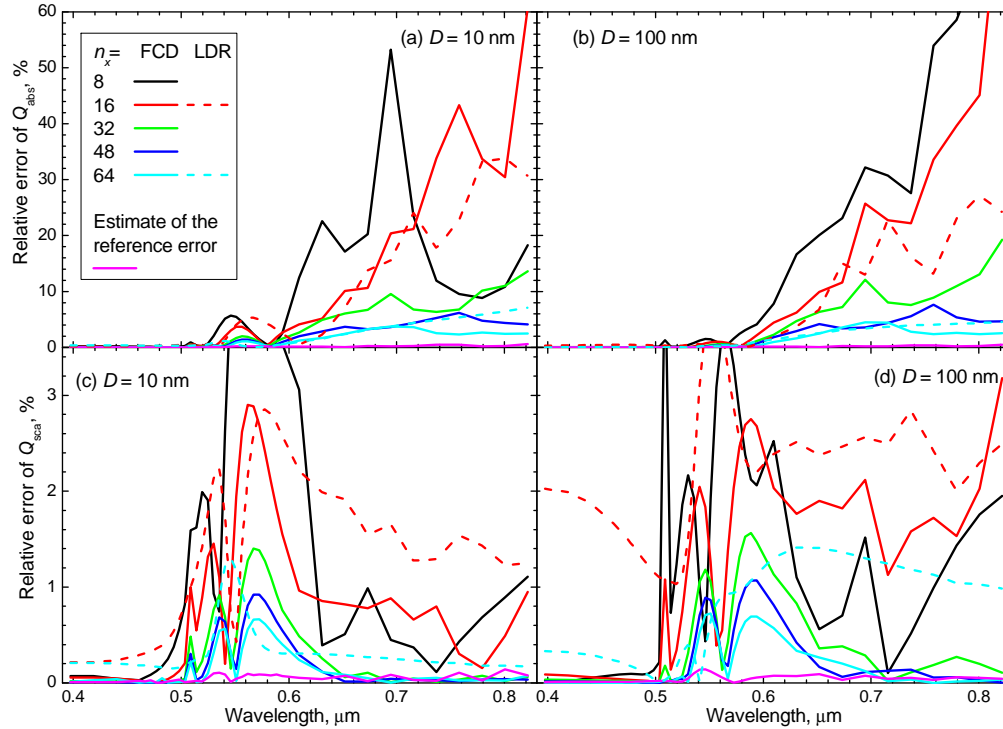


Fig. 3. Relative errors of  $Q_{\text{abs}}$  (a, b) and  $Q_{\text{sca}}$  (c, d) computed using the FCD and LDR formulation of the DDA, varying the number of dipoles, for gold cubes with size 10 nm (a, c) and 100 nm (b, d). Estimated errors of the references are also shown.

the analysis of depolarization factors [60] or equivalently of the spectrum of the DDA interaction matrix [61]. For a Rayleigh sphere this spectrum consists of a single point, while for other shapes it contains at least several points or even a quasi-continuous distribution. In terms of the first factor a rod is closer to a sphere, and in terms of the second to a cube.

Accuracy results for the rod are shown in Fig. 4. The difference in accuracy of  $Q_{\text{abs}}$  and  $Q_{\text{sca}}$  is about a factor two, which is much smaller than for other shapes. Maximum relative errors for the rod are located near the spectral peak, where the convergence of DDA with refining discretization is generally less uniform (this is also true for other shapes), causing oscillations in the error graphs. So we can only conclude that the LDR and FCD have generally comparable accuracy for the rod. Moreover, comparing the accuracy of a particular scattering quantity for the rod to that of spheres or cubes is hampered by the lack of a universal discretization measure. For instance, the latter may be the number of dipoles per the smallest particle dimension ( $n_y$ ) or the total number of dipoles used to discretize the particle ( $\sim n_x n_y^2$ ). If considering the same  $n_y$ ,  $Q_{\text{abs}}$  of the rod is about twice more accurate than that for the sphere, but still much less accurate than that for the cubes. However, the accuracy is comparable if the same total number of dipoles, which determines computational time, is considered. In both cases, accuracy of  $Q_{\text{sca}}$  for the rod is much worse than that for the spheres. From these data we can conclude that the rod is more similar to the spheres than to the cubes in terms of the DDA accuracy. Hence, the influence of particle shape seems to be mostly due to the shape errors, which are the larger part of errors for the rod and the spheres.

Many researchers are interested in the spectral peaks and not in values of  $Q_{\text{abs}}$  or  $Q_{\text{sca}}$  at a particular wavelength. Acknowledging this fact we report the errors of peak position and amplitude in Table 1. Each peak was described by a parabola through three points of the

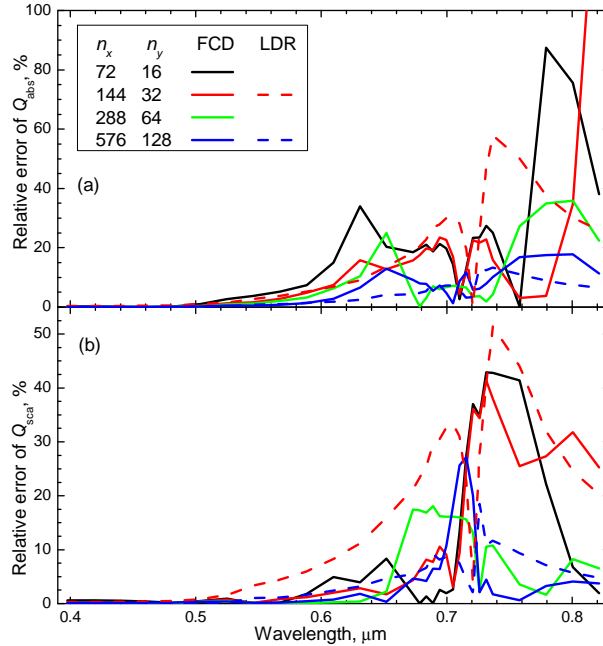


Fig. 4. Relative errors of  $Q_{\text{abs}}$  (a) and  $Q_{\text{sca}}$  (b) computed using the FCD and LDR formulation of the DDA, varying number of dipoles, for a gold rod with size  $20 \times 20 \times 90$  nm (incident polarization is along the rod axis).

spectrum spaced by 5 nm (central point is the maximum one). Errors for absorption and scattering peaks are generally comparable, in contrast to the results for spectra. Errors for the cube and spheres are acceptable even for  $n_x = 32$ , which can be explained by the moderate refractive index in the corresponding wavelength range. Rod shape leads to significantly larger errors, especially considering larger total number of dipoles for the same  $n_y$ . However, it is satisfactory for many practical applications using as small  $n_y$  as 32 ( $n_x = 144$ ). The cubes have the smallest errors, in agreement with the results for spectra. However, the difference between different shapes is not that pronounced. The LDR and the FCD have similar accuracy for the spheres and the cubes, but the situation is markedly different for the rod. The FCD is comparable to the LDR in describing peak position, but has very large errors of peak amplitude. On the contrary, the peak amplitude for the rod computed with the LDR has an accuracy comparable to that for the spheres and cubes. Moreover, the convergence of peak characteristics with discretization is irregular for the rod, which can be explained by the same arguments as used above for Fig. 4.

Computing spectra of nanoparticles with the DDA is an intensive computational task, especially if orientation averaging is required. Computational time for a single orientation depends on the number of iterations and time per iteration. The former is determined mainly by the size and refractive index and the latter by the total number of dipoles [52]. The number of iterations (for one run of the iterative solver) versus wavelength for the spheres ( $n_x = 128$ ) is shown in Fig. 5. The size has only moderate influence on the results, which is expected for particles smaller than the wavelength (in contrast to larger particles [52]). The FCD shows acceleration compared to the LDR from 1.5 to 2 times for  $\lambda > 600$  nm. Results for other shapes are similar (data not shown). Possible reasons for better computational performance of the FCD, in terms of e.g. a more favorable spectrum of the DDA interaction matrix, are discussed elsewhere [47].

Figure 5 also reflects the rapid increase of the computational time with wavelength. Using the FCD, the number of iterations for  $\lambda > 700$  nm is about 20 times larger than for

Table 1. Errors of peak position and amplitude for absorption and scattering spectra.

| shape  | formul.            | $n_y$ | Error of peak position, nm |     |              |     | Relative error of peak amplitude, % |     |              |     |  |
|--------|--------------------|-------|----------------------------|-----|--------------|-----|-------------------------------------|-----|--------------|-----|--|
|        |                    |       | $D = 10$ nm                |     | $D = 100$ nm |     | $D = 10$ nm                         |     | $D = 100$ nm |     |  |
|        |                    |       | abs                        | sca | abs          | sca | abs                                 | sca | abs          | sca |  |
| sphere | FCD                | 32    | 5.8                        | 2.6 | 4.0          | 2.9 | 1.5                                 | 0.8 | 2.6          | 1.3 |  |
|        |                    | 128   | 1.5                        | 0.8 | 1.1          | 0.5 | 0.4                                 | 0.2 | 0.7          | 0.4 |  |
|        | LDR                | 32    | 5.8                        | 2.8 | 4.0          | 2.4 | 1.6                                 | 1.0 | 2.7          | 1.8 |  |
|        |                    | 128   | 1.5                        | 0.7 | 1.0          | 0.6 | 0.4                                 | 0.3 | 0.7          | 0.5 |  |
| cube   | FCD                | 16    | 0.2                        | 1.3 | 1.4          | 0.5 | 0.3                                 | 0.8 | 0.7          | 2.7 |  |
|        |                    | 64    | 0.1                        | 0.0 | 0.5          | 0.2 | 0.1                                 | 0.6 | 0.1          | 0.6 |  |
|        | LDR                | 16    | 0.1                        | 0.8 | 1.1          | 0.4 | 0.6                                 | 2.1 | 0.5          | 2.4 |  |
|        |                    | 64    | 0.2                        | 0.5 | 0.1          | 0.1 | 0.6                                 | 1.1 | 0.2          | 1.0 |  |
|        | rod<br>20×90<br>nm | FCD   | 32                         | abs |              | sca |                                     | abs |              | sca |  |
|        |                    |       | 128                        | 5.0 |              | 5.6 |                                     | 9.8 |              | 22  |  |
| LDR    | 32                 | 7.9   |                            | 8.4 |              | 0.3 |                                     | 2.0 |              |     |  |
|        | 128                | 2.4   |                            | 3.6 |              | 0.6 |                                     | 2.2 |              |     |  |

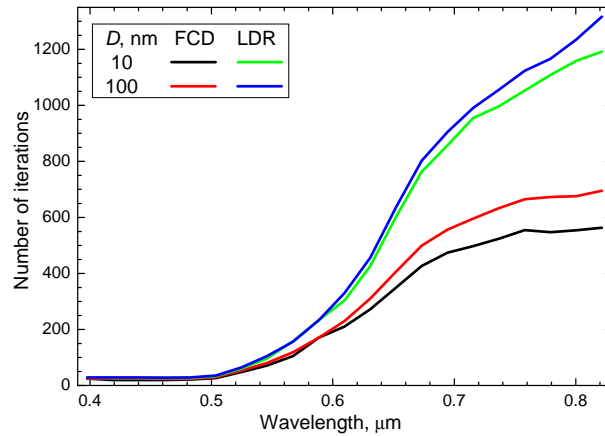


Fig. 5. Number of iterations required by the QMR iterative solver for a gold sphere with diameters 10 nm and 100 nm using the FCD and LDR formulations of the DDA. Stopping criterion  $10^{-5}$  and  $n_x = 128$  were used.

$\lambda < 500$  nm. This problem is further aggravated by the increase of errors with wavelength for fixed discretization (discussed above). If a fixed accuracy is required, larger  $n_x$  should be used for larger wavelengths, resulting in an additional increase of computational time.

All these results support the conclusion that the DDA simulates  $Q_{\text{sca}}$  much more accurately than  $Q_{\text{abs}}$ . We do not have a ready explanation of this fact except for the following hint. For Rayleigh particles light scattering properties are fully determined by the polarizability tensor of the whole particle. In particular, for simulations presented in this manuscript  $Q_{\text{sca}} \sim |\alpha_x|^2$  and  $Q_{\text{abs}} \sim \text{Im}(\alpha_x)$  [55], where  $\alpha_x$  is  $x$ -component of the diagonal polarizability tensor. Therefore, we can conclude that DDA errors of the complex number  $\alpha_x$  are mostly in phase and not in amplitude. However, the exact reasons for that are still unclear.

So far we have discussed  $Q_{\text{abs}}$  and  $Q_{\text{sca}}$  because their accuracy is markedly different, however many practical applications deal with extinction efficiency  $Q_{\text{ext}}$ , which is a sum of the two. The analysis of errors of  $Q_{\text{ext}}$  is hampered by different dependencies of its constituents on size parameter  $x$ :  $Q_{\text{sca}} \sim x^4$  and  $Q_{\text{abs}} \sim x$  (in the Rayleigh regime, [55]).



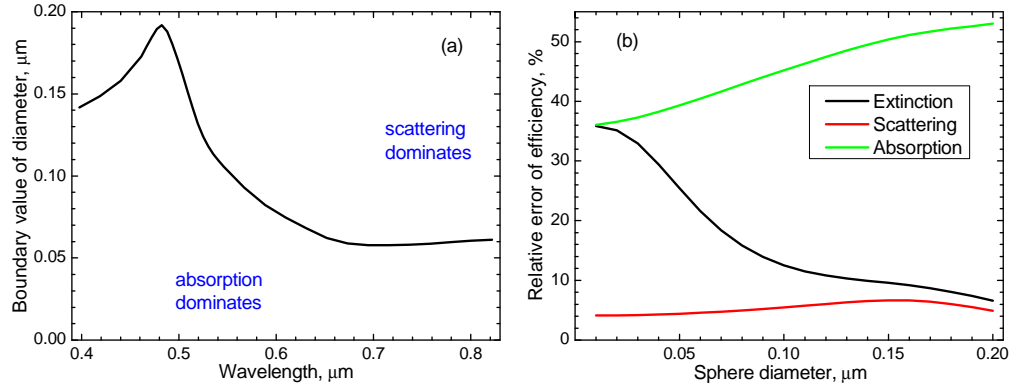


Fig. 6. (a) Boundary value of diameter of a gold sphere, for which  $Q_{\text{abs}} = Q_{\text{sca}}$ , versus wavelength. (b) Relative errors of  $Q_{\text{ext}}$ ,  $Q_{\text{sca}}$ , and  $Q_{\text{abs}}$  of a gold sphere computed using the FCD formulation of DDA as a function of sphere diameter. Wavelength 0.694  $\mu\text{m}$  ( $m = 0.129 + 4.01i$ ) and  $n_x = 64$  were used.

Therefore,  $Q_{\text{sca}} \ll Q_{\text{abs}}$  for  $x \ll 1$ , and vice versa for  $x \sim 1$ . The boundary value of sphere diameter, for which  $Q_{\text{sca}} = Q_{\text{abs}}$ , is shown in Fig. 6(a) versus wavelength. This boundary is in the middle of the typical size range of gold nanoparticles. Therefore, the relative errors of  $Q_{\text{ext}}$  strongly depend on the particle size – it is similar to that of  $Q_{\text{abs}}$  and  $Q_{\text{sca}}$  for smaller and larger particles respectively. For example, this behavior for a particular wavelength (0.694  $\mu\text{m}$ ) is shown in Fig. 6(b). It is important to note that size dependence of both  $Q_{\text{abs}}$  and  $Q_{\text{sca}}$  is much less pronounced than that of  $Q_{\text{ext}}$ . In this particular respect (concerning DDA accuracy), absorption and scattering seem to be more fundamental than extinction. Moreover, Fig. 6(b) explains why very large errors of  $Q_{\text{abs}}$  were not noticed in studies calculating the extinction spectrum of relatively large particles (e.g. 300 nm spheres, [37]).

Another quantity, relevant for certain applications, is radiation pressure efficiency  $Q_{\text{pr}}$  [62]. However, it is approximately equal to  $Q_{\text{ext}}$  for particles smaller than the wavelength [55]. Therefore, we do not discuss it separately in this manuscript.

## 4 CONCLUSION

The main general conclusion is that caution should be exercised when the DDA is applied to simulate optical properties of gold nanoparticles. It can successfully predict position and amplitudes of spectral peaks, using moderate discretization (32 dipoles per shortest particle dimension). However, a much finer discretization (4-8 smaller dipole size) is required to keep the relative error of  $Q_{\text{abs}}$  in the wavelength range [600,800] nm within 10%. Therefore, an accuracy study of DDA for a particular application is advised to achieve a compromise between computational speed and accuracy of a specific scattering quantity. Universally accurate DDA results may be too computationally expensive to compute.

The largest errors are observed for  $Q_{\text{abs}}$  of the spheres and the rod. Fortunately, the errors for the cubes are an order of magnitude smaller for the same dipole size. Supposedly, the situation is similar for other shapes that can be exactly described by a set of cubical dipoles due to absence of shape errors. For other shapes the accuracy of DDA may be significantly improved by employing weighted discretization of the particle surface [63]. However, this improvement has not been yet implemented in any publicly available DDA code, and hence is left for future research.

The relative errors of  $Q_{\text{sca}}$  are about 10 times less than that of  $Q_{\text{abs}}$  for the spheres and the cubes, but only 2 times for the rod. Accuracy of  $Q_{\text{ext}}$  is similar to that of  $Q_{\text{abs}}$  for smaller and to that of  $Q_{\text{sca}}$  for larger particles. The boundary diameter for the spheres is 50-200 nm in the

wavelength range [400,800] nm. Therefore, accuracy of  $Q_{\text{ext}}$  can be unusually poor for sufficiently small nanoparticles.

We compared two DDA formulations: the FCD and the LDR. None of them can claim conclusive superiority in terms of accuracy, although the FCD is generally more accurate. However, the FCD results in up to 2 times faster convergence of the iterative solver. Therefore, we recommend using the FCD instead of the standard LDR for gold nanoparticles, which is facilitated by the fact that the former is implemented in the publicly available code ADDA.

We considered all test gold particles in vacuum, which may lead to certain exaggeration of the problems with DDA accuracy as compared to particles in water. However, all conclusions should hold for the latter. Moreover, similar conclusions are expected to be true for the silver nanoparticles due to the similar refractive index spectrum, although it would be a subject of further study.

## 5 IN HONOR OF CRAIG BOHREN

As this paper will appear in a special issue, dedicated to 70th birthday of Craig F. Bohren, one of the authors (AgH) wishes to spend a few words on some good memories. It was in 1991 that I met Craig Bohren during the Optical Particle Sizing conference in Tempe, Arizona. Craig Bohren was sitting in front of the room, making many notes and at the end of the meeting he was asked by the organizer (Dan Hirleman) to provide a summary. Craig did that by making many (very) critical remarks, and then ending his summary with "If I failed to offend you all, I apologize". I just started as a PhD student and this made a deep impression on me. Together with Peter Sloot I joined a post-conference trip to the Grand Canyon (for pictures of participants, see *Applied Optics*, vol. 30, nr 33, 1991, page 4687). We were in a minivan together with Craig Bohren, Henk van der Hulst, and Dan Hirleman. While driving we saw this beautiful rainbow. We stopped the car, and admired it, using our Polaroid sunglasses to observe the polarization. This made an even bigger impression, being amidst these giants of the light scattering community, together observing a rainbow. I guess one of the reasons that I am still in science is this great moment at the start of my career.

We wish to congratulate Craig Bohren and thank him for the deep impact that he and his work has made on us.

## Acknowledgments

We acknowledge illuminating discussions with Baptiste Auguie, Rick Harrison, and George C. Schatz. Konstantin V. Gilev is gratefully acknowledged for modifying the T-matrix code for our needs. We thank anonymous reviewers for their comments and suggestions to improve the manuscript.

MaY is supported by grants of the Russian Foundation for Basic Research, No 07-04-00356-a, and No 08-02-91954-NNIO\_a, integration grants of the Siberian Branch of the Russian Academy of Science, No 2009-37, and No 2009-7, grant from the program of Presidium of the Russian Academy of Science, No 2009-27b, and by program of the Russian Government "Research and educational personnel of innovative Russia" (contract P2497).

## References

- [1] N. G. Khlebtsov, "Optics and biophotonics of nanoparticles with a plasmon resonance," *Quant. Electron.* **38**, 504-529 (2008) [doi:10.1070/QE2008v038n06ABEH013829].
- [2] X. Lu, M. Rycenga, S. E. Skrabalak, B. Wiley, and Y. Xia, "Chemical synthesis of novel plasmonic nanoparticles," *Ann. Rev. Phys. Chem.* **60**, 167-192 (2009) [doi:10.1146/annurev.physchem.040808.090434].

- [3] I. Pastoriza-Santos and L. M. Liz-Marzan, "Colloidal silver nanoplates. State of the art and future challenges," *J. Mater. Chem.* **18**, 1724-1737 (2008) [doi:10.1039/b716538b].
- [4] S. Eustis and M. A. El-Sayed, "Why gold nanoparticles are more precious than pretty gold: Noble metal surface plasmon resonance and its enhancement of the radiative and nonradiative properties of nanocrystals of different shapes," *Chem. Soc. Rev.* **35**, 209-217 (2006) [doi:10.1039/b514191e].
- [5] K. A. Bosnick, J. Jiang, and L. E. Brus, "Fluctuations and local symmetry in single-molecule rhodamine 6G Raman scattering on silver nanocrystal aggregates," *J. Phys. Chem. B* **106**, 8096-8099 (2002) [doi:10.1021/jp0256241].
- [6] J. Lakowicz, C. Geddes, I. Gryczynski, J. Malicka, Z. Gryczynski, K. Aslan, J. Lukomska, E. Matveeva, J. Zhang, R. Badugu, and J. Huang, "Advances in surface-enhanced fluorescence," *J. Fluoresc.* **14**, 425-441 (2004) [doi:10.1023/B:JOFL.0000031824.48401.5c].
- [7] S. D'Agostino, P. P. Pompa, R. Chiuri, R. J. Phaneuf, D. G. Britti, R. Rinaldi, R. Cingolani, and F. Della Sala, "Enhanced fluorescence by metal nanospheres on metal substrates," *Opt. Lett.* **34**, 2381-2383 (2009) [doi:10.1364/OL.34.002381].
- [8] S. Kumar, N. Harrison, R. Richards-Kortum, and K. Sokolov, "Plasmonic nanosensors for imaging intracellular biomarkers in live cells," *Nano Lett.* **7**, 1338-1343 (2007) [doi:10.1021/nl070365i].
- [9] I. H. El-Sayed, X. Huang, and M. A. El-Sayed, "Selective laser photo-thermal therapy of epithelial carcinoma using anti-EGFR antibody conjugated gold nanoparticles," *Cancer Lett.* **239**, 129-135 (2006) [doi:10.1016/j.canlet.2005.07.035].
- [10] M. E. Stewart, C. R. Anderton, L. B. Thompson, J. Maria, S. K. Gray, J. A. Rogers, and R. G. Nuzzo, "Nanostructured plasmonic sensors," *Chem. Rev.* **108**, 494-521 (2008) [doi:10.1021/cr068126n].
- [11] H. Yoo, J. E. Millstone, S. Li, J. Jang, W. Wei, J. Wu, G. C. Schatz, and C. A. Mirkin, "Core-shell triangular bifrustums," *Nano Lett.* **9**, 3038-3041 (2009) [doi:10.1021/nl901513g].
- [12] M. D. Malinsky, K. L. Kelly, G. C. Schatz, and R. P. Van Duyne, "Nanosphere lithography: effect of substrate on the localized surface plasmon resonance spectrum of silver nanoparticles," *J. Phys. Chem. B* **105**, 2343-2350 (2001) [doi:10.1021/jp002906x].
- [13] P. Muhlschlegel, H. Eisler, O. J. F. Martin, B. Hecht, and D. W. Pohl, "Resonant optical antennas," *Science* **308**, 1607-1609 (2005) [doi:10.1126/science.1111886].
- [14] T. Jensen, L. Kelly, A. Lazarides, and G. C. Schatz, "Electrodynamics of noble metal nanoparticles and nanoparticle clusters," *J. Clust. Sci.* **10**, 295-317 (1999) [doi:10.1023/A:1021977613319].
- [15] V. Myroshnychenko, J. Rodriguez-Fernandez, I. Pastoriza-Santos, A. M. Funston, C. Novo, P. Mulvaney, L. M. Liz-Marzan, and F. J. G. D. Abajo, "Modelling the optical response of gold nanoparticles," *Chem. Soc. Rev.* **37**, 1792-1805 (2008) [doi:10.1039/b711486a].
- [16] C. Noguez, "Surface plasmons on metal nanoparticles: The influence of shape and physical environment," *J. Phys. Chem. C* **111**, 3606-3619 (2007) [doi:10.1021/jp066539m].
- [17] V. Myroshnychenko, E. Carbó-Argibay, I. Pastoriza-Santos, J. Pérez-Juste, L. M. Liz-Marzán, and F. J. G. D. Abajo, "Modeling the optical response of highly faceted metal nanoparticles with a fully 3D boundary element method," *Adv. Mater.* **20**, 4288-4293 (2008) [doi:10.1002/adma.200703214].
- [18] A. M. Kern and O. J. F. Martin, "Surface integral formulation for 3D simulations of plasmonic and high permittivity nanostructures," *J. Opt. Soc. Am. A* **26**, 732-740 (2009) [doi:10.1364/JOSAA.26.000732].

- [19] J. Hellmers, N. Riefler, T. Wriedt, and Y. A. Eremin, "Light scattering simulation for the characterization of sintered silver nanoparticles," *J. Quant. Spectrosc. Radiat. Trans.* **109**, 1363-1373 (2008) [doi:10.1016/j.jqsrt.2007.10.009].
- [20] T. Wriedt, "Review of the null-field method with discrete sources," *J. Quant. Spectrosc. Radiat. Trans.* **106**, 535-545 (2007) [doi:10.1016/j.jqsrt.2007.01.043].
- [21] F. Hao, C. L. Nehl, J. H. Hafner, and P. Nordlander, "Plasmon resonances of a gold nanostar," *Nano Lett.* **7**, 729-732 (2007) [doi:10.1021/nl062969c].
- [22] C. Ungureanu, R. G. Rayavarapu, S. Manohar, and T. G. van Leeuwen, "Discrete dipole approximation simulations of gold nanorod optical properties: Choice of input parameters and comparison with experiment," *J. Appl. Phys.* **105**, 102032-7 (2009) [doi:10.1063/1.3116139].
- [23] W. H. Yang, G. C. Schatz, and R. P. Vandyne, "Discrete dipole approximation for calculating extinction and Raman intensities for small particles with arbitrary shapes," *J. Chem. Phys.* **103**, 869-875 (1995) [doi:10.1063/1.469787].
- [24] K. L. Kelly, E. Coronado, L. Zhao, and G. C. Schatz, "The optical properties of metal nanoparticles: the influence of size, shape, and dielectric environment," *J. Phys. Chem. B* **107**, 668-677 (2003) [doi:10.1021/jp026731y].
- [25] "ADDA – light scattering simulator using the discrete dipole approximation," <http://code.google.com/p/a-dda/> (2009).
- [26] "DDSCAT – the discrete dipole approximation for scattering and absorption of light by irregular particles," <http://www.astro.princeton.edu/~draine/DDSCAT.html> (2009).
- [27] C. Girard, A. Dereux, O. J. F. Martin, and M. Devel, "Importance of confined fields in near-field optical imaging of subwavelength objects," *Phys. Rev. B* **50**, 14467-14473 (1994) [doi:10.1103/PhysRevB.50.14467].
- [28] S. Guo, S. Tsai, H. Kan, D. Tsai, M. R. Zachariah, and R. J. Phaneuf, "The effect of an active substrate on nanoparticle-enhanced fluorescence," *Adv. Mater.* **20**, 1424-1428 (2008) [doi:10.1002/adma.200701126].
- [29] E. Bae and E. D. Hirleman, "Extending the applicability of the discrete dipole approximation for multi-scale features on surface," *J. Quant. Spectrosc. Radiat. Trans.* **107**, 470-478 (2007) [doi:10.1016/j.jqsrt.2007.03.001].
- [30] P. C. Chaumet, A. Rahmani, and G. W. Bryant, "Generalization of the coupled dipole method to periodic structures," *Phys. Rev. B* **67**, 165404 (2003) [doi:10.1103/PhysRevB.67.165404].
- [31] S. Zou, N. Janel, and G. C. Schatz, "Silver nanoparticle array structures that produce remarkably narrow plasmon lineshapes," *J. Chem. Phys.* **120**, 10871-10875 (2004) [doi:10.1063/1.1760740].
- [32] B. T. Draine and P. J. Flatau, "Discrete-dipole approximation for periodic targets: theory and tests," *J. Opt. Soc. Am. A* **25**, 2693-2703 (2008) [doi:10.1364/JOSAA.25.002693].
- [33] C. Pecharroman, J. Perez-Juste, G. Mata-Osoro, L. M. Liz-Marzan, and P. Mulvaney, "Redshift of surface plasmon modes of small gold rods due to their atomic roughness and end-cap geometry," *Phys. Rev. B* **77**, 035418 (2008) [doi:10.1103/PhysRevB.77.035418].
- [34] E. Hao, G. Schatz, and J. Hupp, "Synthesis and optical properties of anisotropic metal nanoparticles," *J. Fluores.* **14**, 331-341 (2004) [doi:10.1023/B:JOFL.0000031815.71450.74].
- [35] J. E. Millstone, S. Park, K. L. Shuford, L. Qin, G. C. Schatz, and C. A. Mirkin, "Observation of a quadrupole plasmon mode for a colloidal solution of gold nanoprisms," *J. Amer. Chem. Soc.* **127**, 5312-5313 (2005) [doi:10.1021/ja043245a].

- [36] E. S. Kooij and B. Poelsema, "Shape and size effects in the optical properties of metallic nanorods," *Phys. Chem. Chem. Phys.* **8**, 3349-3357 (2006) [doi:10.1039/b518389h].
- [37] K. L. Shuford, M. A. Ratner, and G. C. Schatz, "Multipolar excitation in triangular nanoprisms," *J. Chem. Phys.* **123**, 114713 (2005) [doi:10.1063/1.2046633].
- [38] K. Lee and M. A. El-Sayed, "Dependence of the enhanced optical scattering efficiency relative to that of absorption for gold metal nanorods on aspect ratio, size, end-cap shape, and medium refractive index," *J. Phys. Chem. B* **109**, 20331-20338 (2005) [doi:10.1021/jp054385p].
- [39] P. Yang, H. Portalès, and M. Pileni, "Identification of multipolar surface plasmon resonances in triangular silver nanoprisms with very high aspect ratios using the DDA method," *J. Phys. Chem. C* **113**, 11597-11604 (2009) [doi:10.1021/jp901248e].
- [40] I. O. Sosa, C. Noguez, and R. G. Barrera, "Optical properties of metal nanoparticles with arbitrary shapes," *J. Phys. Chem. B* **107**, 6269-6275 (2003) [doi:10.1021/jp0274076].
- [41] P. K. Jain, K. S. Lee, I. H. El-Sayed, and M. A. El-Sayed, "Calculated absorption and scattering properties of gold nanoparticles of different size, shape, and composition: applications in biological imaging and biomedicine," *J. Phys. Chem. B* **110**, 7238-7248 (2006) [doi:10.1021/jp057170o].
- [42] B. T. Draine and J. J. Goodman, "Beyond clausius-mossotti - wave-propagation on a polarizable point lattice and the discrete dipole approximation," *Astrophys. J.* **405**, 685-697 (1993) [doi:10.1086/172396].
- [43] D. Gutkowitz-Krusin and B. T. Draine, "Propagation of electromagnetic waves on a rectangular lattice of polarizable points," (2004) <http://arxiv.org/abs/astro-ph/0403082>.
- [44] N. B. Piller and O. J. F. Martin, "Increasing the performance of the coupled-dipole approximation: A spectral approach," *IEEE Trans. Antennas Propagat.* **46**, 1126-1137 (1998) [doi:10.1109/8.718567].
- [45] P. C. Chaumet, A. Sentenac, and A. Rahmani, "Coupled dipole method for scatterers with large permittivity," *Phys. Rev. E* **70**, 036606 (2004) [doi:10.1103/PhysRevE.70.036606].
- [46] M. A. Yurkin and A. G. Hoekstra, "The discrete dipole approximation: an overview and recent developments," *J. Quant. Spectrosc. Radiat. Trans.* **106**, 558-589 (2007) [doi:10.1016/j.jqsrt.2007.01.034].
- [47] M. A. Yurkin, M. Min, and A. G. Hoekstra, "Application of the discrete dipole approximation to extreme refractive indices: filtered coupled dipoles revived," to be submitted to *Optics Express* (2010).
- [48] P. B. Johnson and R. W. Christy, "Optical constants of the noble metals," *Phys. Rev. B* **6**, 4370 (1972) [doi:10.1103/PhysRevB.6.4370].
- [49] E. M. Purcell and C. R. Pennypacker, "Scattering and adsorption of light by nonspherical dielectric grains," *Astrophys. J.* **186**, 705-714 (1973) [doi:10.1086/152538].
- [50] B. T. Draine and P. J. Flatau, "Discrete-dipole approximation for scattering calculations," *J. Opt. Soc. Am. A* **11**, 1491-1499 (1994) [doi:10.1364/JOSAA.11.001491].
- [51] G. H. Goedecke and S. G. O'Brien, "Scattering by irregular inhomogeneous particles via the digitized Green's function algorithm," *Appl. Opt.* **27**, 2431-2438 (1988) [doi:10.1364/AO.27.002431].
- [52] M. A. Yurkin, V. P. Maltsev, and A. G. Hoekstra, "The discrete dipole approximation for simulation of light scattering by particles much larger than the

- wavelength," *J. Quant. Spectrosc. Radiat. Trans.* **106**, 546-557 (2007) [doi:10.1016/j.jqsrt.2007.01.033].
- [53] R. W. Freund, "Conjugate gradient-type methods for linear-systems with complex symmetrical coefficient matrices," *SIAM J. Sci. Stat. Comp.* **13**, 425-448 (1992) [doi:10.1137/0913023].
- [54] "Description of the national compute cluster Lisa," <https://subtrac.sara.nl/userdoc/wiki/lisa/description> (2009).
- [55] C. F. Bohren and D. R. Huffman, *Absorption and Scattering of Light by Small Particles*, Wiley, New York (1983).
- [56] M. I. Mishchenko and L. D. Travis, "Capabilities and limitations of a current FORTRAN implementation of the T-matrix method for randomly oriented, rotationally symmetric scatterers," *J. Quant. Spectrosc. Radiat. Trans.* **60**, 309-324 (1998) [doi:10.1016/S0022-4073(98)00008-9].
- [57] M. I. Mishchenko, "Calculation of the amplitude matrix for a nonspherical particle in a fixed orientation," *Appl. Opt.* **39**, 1026-1031 (2000) [doi:10.1364/AO.39.001026].
- [58] M. A. Yurkin, V. P. Maltsev, and A. G. Hoekstra, "Convergence of the discrete dipole approximation. II. An extrapolation technique to increase the accuracy," *J. Opt. Soc. Am. A* **23**, 2592-2601 (2006) [doi:10.1364/JOSAA.23.002592].
- [59] M. I. Mishchenko, L. D. Travis, and A. A. Lacis, *Scattering, Absorption, and Emission of Light by Small Particles*, Cambridge University Press, Cambridge (2002).
- [60] R. Fuchs, "Theory of the optical properties of ionic crystal cubes," *Phys. Rev. B* **11**, 1732-1740 (1975) [doi:10.1103/PhysRevB.11.1732].
- [61] M. Min, J. W. Hovenier, A. Dominik, A. de Koter, and M. A. Yurkin, "Absorption and scattering properties of arbitrary shaped particles in the Rayleigh domain: A rapid computational method and a theoretical foundation for the statistical approach," *J. Quant. Spectrosc. Radiat. Trans.* **97**, 161-180 (2006) [doi:10.1016/j.jqsrt.2005.05.059].
- [62] A. G. Hoekstra, M. Frijlink, L. B. F. M. Waters, and P. M. A. Sloot, "Radiation forces in the discrete-dipole approximation," *J. Opt. Soc. Am. A* **18**, 1944-1953 (2001) [doi:10.1364/JOSAA.18.001944].
- [63] N. B. Piller, "Influence of the edge meshes on the accuracy of the coupled-dipole approximation," *Opt. Lett.* **22**, 1674-1676 (1997) [doi:10.1364/OL.22.001674].

**Maxim A. Yurkin** is a researcher at the Institute of Chemical Kinetics and Combustion. He received his BS and MS degrees in physics with honors from the Novosibirsk State University in 2002 and 2004, respectively. He received two PhD degrees: in computational science from the University of Amsterdam in 2007 and in biophysics from Institute of Chemical Kinetics and Combustion (Novosibirsk) in 2008. He is the author of more than 15 journal papers and two book chapters. His current research interests include the discrete dipole approximation, inverse light-scattering problems, and characterization of blood cells. He received young scientist's award in electromagnetic and light scattering by Elsevier in 2007.

**David de Kanter holds a M.Sc. in Physics from the University of Amsterdam. Currently he** is a scientific programmer at the University of Amsterdam. Since 2004 he provides technical support for the light scattering research. He made light scattering simulations for models of white blood cells and gold nanoparticles using the discrete dipole approximation (DDA) at the computing cluster LISA at SARA in Amsterdam, and has co-authored 3 publications on this subject.

**Alfons G. Hoekstra** holds PhD in Computational Physics from the University of Amsterdam. Currently he is an Associate Professor in the Computational Sciences at the University of Amsterdam. His research interest lies in modeling and simulation of multi-scale multi-physics systems, with special emphasis on the biomedical domain. He has published over a 100 research papers, edited several books, and organized workshops and conferences on high performance computing, grid computing, light scattering, cellular automata, and mesoscopic methods for fluid dynamics.